IIETA International Information and Engineering Technology Association
Advancing the World of Information and Engineering

TECNICA ITALIANA-Italian Journal of Engineering Science
Vol. 61+1, No. 1, June, 2018, pp. 12-21
Journal homepage: http://iieta.org/Journals/TI-IJES

Cattaneo-Christov heat flux on UCM flow across a melting surface with cross diffusion and double stratification

Shaik M. Ibrahim[1], Fazle Mabood[2], Prathi V. Kumar[1], Giulio Lorenzini[3], Enrico Lorenzini[4*]

[1] Dept. of Mathematics, GITAM University, Visakhapatnam, Andhra Pradesh-530045, India
[2] Department of Mathematics, University of Peshawar, Pakistan
[3] Department of Engineering and Architecture, University of Parma, Parco Area delle Scienze 181/A, 43124 Parma, Italy
[4] Alma Mater Studiorum-University of Bologna, Department of Industrial Engineering, viale Risorgimento no.2, Bologna 40136, Italy

Corresponding Author Email: giulio.lorenzini@unipr.it

https://doi.org/10.18280/ti-ijes.620102

Received: 7 January 2018
Accepted: 15 March 2018

Keywords:
Cattaneo-Christov, heat flux model, UCM fluid, helting surface, brownian motion and thermophoresis, thermal stratification parameter, solutal stratification parameter, viscous parameter

ABSTRACT

The theoretical is investigation is performed for Cattaneo-Christov heat flux on UCM fluid over a melting surface in the presence of exponentially decaying heat source or sink. Melting surfaces have major real-time applications such as industrial and manufacturing processes (Pharma, beverage's and leather industries). We also incorporated the cross diffusion and double thermal stratifications effects for controlling the heat and mass transfer phenomena. The governing system of partial differential equations (PDEs) is transformed into non-linear ordinary differential equations (ODEs) and which answered by using fourth-fifth Runge Kutta Felhberg -integration scheme. We also calculated the local Nusselt and Sherwood number values as well as velocity, temperature and concentration profiles for various physical governing parameters such as exponentially decaying heat source or sink, thermal stratification, Soret and dufour numbers. It is found that the thermal relaxation helps to improve the local Nusselt number whereas thermal stratification enhances the mass transfer rate.

1. INTRODUCTION

During the past decade, a new heat flux model as Cattaneo-Christov has attracted enormous interest in heat transfer that happen in the formation of thermal waves. Evolving this model in the thermal equation gives us the differential equation of type hyperbolic. Earlier, Cattaneo [1] proposed a good model by extended the Fourier's law due to the thermal relaxation of time only. Further, Maxwell Cattaneo model of finite speed conduction of heat with the help in different frame formulations has been developed by Christov [2]. Mustafa [3] initiated a rotating flow and heat transfer of UCM with Cattaneo-Christov heat flux model in the presence of different geometries. A rotating flow 3-D Jeffrey fluid with Cattaneo-Christov heat flux model developed by Hayat et al. [4]. On the same characteristics peristalsis flow of different geometries of Cattaneo-Christov heat flux model developed by Tanveer et al. [5]. A very rare developed model considered numerical investigation with viscoelastic model for Cattaneo-Christov heat flux due to an exponentially stretching sheet computed by Junaid et al. [6]. Recently, the researchers [7-10] used UCM with Cattaneo-Christov heat flux model in their heat transfer characteristics of different geometries. It is also a great significance to adopt a respective domain which is relatively applications in real life situations.

The study of double-diffusive convection has considered during the past years its occurrence in wide range of technological and natural settings. Double diffusive convection is a reliable fluid dynamic phenomenon that involves a common example in oceanography, where heat and salt concentrations with different gradients and diffusive free convection is also seen in sea-wind formations, where upward convection is also modified by Coriolis forces. Its convection has also important role in modeling has also important role in modeling of Magma chambers [11-12] and solar ponds [13]. In engineering areas, double diffusive convection has visualized in the form of fluid flows and molten metals surrounded by heat-dissipation fins. Narayana et al. [16] and Malashetty et al. [17] have developed the double and cross diffusive effects binary Maxwell fluid due porous surface. The behaviour of laminar double diffusive flow of a viscous Newtonian fluidIn in a titled square enclouser filled with a non-Darcian porous medium inunder heat generation or absorption was studied by Chamkha and Abdulgafoor [18]. Nasrin and Alim [19] analysed the Soret and Dufour effects on natural convection flow in a partially heated square chamber. Ghernaout et al. [20] obtained the numerical results of double diffusive natural convection in binary mixture under the effect of external magnetic field for the steady and the oscillatory state. Al-Humoud and Chamkha [21] studied the double diffusive convection of rotating fluid over a surface embedded in a thermally stratified hogh-porosity medium. In recent years, many researchers have investigated some flow parameters on cross diffusion and double stratification [22-25].

The present work aims to fill the gap in the existing literature. In this present letter, we extended the work by Adegbie et al. [26] due to conclude the study of Cattaneo-Christov heat flux with cross diffusion and double stratification. The model is first constructed and then similarity solutions are obtained numerical investigated through

shooting approximation.

2. MATHEMATICAL FORMULATION

We consider an incompressible, steady two dimensional Upper Convicted Maxwell fluid (UCM) across a melting surface located in hot surroundings. We assumed that the normal stress and shear stress are of the same order of magnitude. We have considered temperature dependent thermal conductivity as $\mu(\mathrm{T}) = \mu\lfloor a_1 + b_1(T_\infty - T)\rfloor$ and viscous parameter as $\mu(\mathrm{T}) = \mu\lfloor a_1 + b_1(T_\infty - T)\rfloor$. We applied the usual boundary layer theory estimations to simply the momentum and energy equations.

The governing equations are

$$\frac{\partial u}{\partial x} + \frac{\partial v}{\partial y} = 0, \tag{1}$$

$$\begin{aligned} &u\frac{\partial u}{\partial x} + v\frac{\partial u}{\partial y} + \lambda\left(u^2\frac{\partial^2 u}{\partial x^2} + v^2\frac{\partial^2 u}{\partial y^2} + 2uv\frac{\partial^2 u}{\partial x \partial y}\right), \\ &= \frac{1}{\rho}\frac{\partial}{\partial y}\left(\mu\frac{\partial u}{\partial y}\right) - \frac{\sigma B^2}{\rho}\left(u + \lambda v\frac{\partial u}{\partial y}\right) \end{aligned} \tag{2}$$

$$\begin{aligned} u\frac{\partial T}{\partial x} + v\frac{\partial T}{\partial y} &= \frac{1}{\rho c_p}\frac{\partial}{\partial y}\left(k\frac{\partial u}{\partial y}\right) + \frac{Q_0\left(T_\infty - T\right)}{\rho c_p}e^{-ny\sqrt{\frac{a}{c}}} \\ &+ \frac{D_m k_T}{c_s c_p}\frac{\partial^2 C}{\partial y^2} + \lambda_2\begin{pmatrix} u\frac{\partial u}{\partial x}\frac{\partial T}{\partial x} + v\frac{\partial v}{\partial y}\frac{\partial T}{\partial y} + u\frac{\partial u}{\partial x}\frac{\partial T}{\partial y} \\ + v\frac{\partial u}{\partial y}\frac{\partial T}{\partial x} + 2uv\frac{\partial^2 T}{\partial x \partial y} \\ + u^2\frac{\partial^2 T}{\partial y^2} + v^2\frac{\partial^2 T}{\partial y^2} \end{pmatrix}, \end{aligned} \tag{3}$$

$$u\frac{\partial C}{\partial x} + v\frac{\partial C}{\partial y} = D_m\frac{\partial^2 C}{\partial y^2} + \frac{D_m k_T}{T_m}\frac{\partial^2 T}{\partial y^2}, \tag{4}$$

Subject to the boundary conditions

$$\left.\begin{aligned} &u = 0,\ k^*\left(\frac{\partial T}{\partial y}\right) = \rho\left[\lambda^* + c_s\left(T_m - T_0^*\right)v\right], \\ &T = T_m = T_0 + m_1 x,\ C = C_m = C_0 + m_3 x \end{aligned}\right\} \ at\ y = 0, \tag{5}$$

$$\left.\begin{aligned} &u \to u_e(= ax),\ T \to T_\infty = T_0 + m_2 x, \\ &C \to C_\infty = C_0 + m_4 x \end{aligned}\right\} \ as\ y \to \infty.$$

With the aid of the below transformations, the Eq (1) to Eq (4) transformed as the set of non-linear ordinary differential equations:

$$\begin{aligned} &u = ax\frac{df}{d\zeta},\ v = -\sqrt{a\nu}\,f(\zeta), \theta(\zeta) = \frac{T - T_m}{T_\infty - T_0} \\ &\phi(\zeta) = \frac{C - C_m}{C_\infty - C_0}, \zeta = y\sqrt{\frac{a}{\nu}} \end{aligned} \tag{6}$$

With the help of (6), Eq (2) to Eq (5) transmuted as the following equations:

$$\begin{aligned} &\left[a_1 + (1 - \theta - S_t)\xi - \beta f^2\right]\frac{d^3 f}{d\zeta^3} \\ &+ \left(f - \xi\frac{d\theta}{d\zeta} + 2\beta f\frac{df}{d\zeta} + M\beta f\right)\frac{d^2 f}{d\zeta^2} \\ &- \left(\frac{df}{d\zeta} + M\right)\frac{df}{d\zeta} = 0 \end{aligned} \tag{7}$$

$$\begin{aligned} &\left[a_2 + \varepsilon\theta\right]\frac{d^2\theta}{d\zeta^2} + \varepsilon\left(\frac{df}{d\zeta}\right)^2 - Pr\,S_t\frac{df}{d\zeta} \\ &+ Pr\,\theta\frac{df}{d\zeta} + Pr\,f\frac{d\theta}{d\zeta} + Pr\,\delta e^{-n\zeta} + Pr\,Du\frac{d^2\phi}{d\zeta^2} \\ &- \gamma\left(f\frac{d\theta}{d\zeta}\frac{df}{d\zeta} + f^2\frac{d^2\theta}{d\zeta^2}\right) = 0 \end{aligned} \tag{8}$$

$$\frac{d^2\phi}{d\zeta^2} - Sc\left(\frac{d\phi}{d\zeta} - f\frac{d\phi}{d\zeta} + S_{sol}\frac{df}{d\zeta} - Sr\frac{d^2\phi}{d\zeta^2}\right) = 0 \tag{9}$$

And the boundary conditions Eq (5) changed as

$$\begin{aligned} &m\frac{df}{d\zeta} + Pr\,f\Big|_{\zeta=0}, \frac{df}{d\zeta}\Big|_{\zeta=0} = 0, \theta(0) = 0, \phi(0) = 0, \\ &\frac{df}{d\zeta}\Big|_{\zeta=\infty} = 1, \theta(\infty) = (1 - S_t), \phi(\infty) = (1 - S_{sol}). \end{aligned} \tag{10}$$

where $S_t, \xi, \beta, M, \varepsilon, Pr, \gamma, \delta, Du, Sc, Sr$ and m are defined as

$$\begin{aligned} &S_t = \frac{T_m - T_0}{T_\infty - T_0}, \xi = b_1(T_\infty - T_0), \beta = \lambda a, M = \frac{\sigma B^2}{a\rho}, \\ &\gamma = \lambda_2 a, Sr = \frac{D_m k_T(T_\infty - T_0)}{\nu T_m(C_\infty - C_0)}, Sc = \frac{\nu}{D_m}, \\ &\varepsilon = b_2(T_\infty - T_0), Pr = \frac{\mu C_p}{k}, Du = \frac{D_m k_T(C_\infty - C_0)}{\nu c_s c_p T_m(T_\infty - T_0)}, \\ &m = \frac{C_p(T_\infty - T_0)}{\left[\lambda^* + c_s\left(T_m - T_0^*\right)\right]}, \delta = \frac{Q_0}{\rho C_p a}. \end{aligned} \tag{11}$$

The skin friction coefficient Cf, the local Nusselt number Nu_x and the local Sherwood number Sh_x are specified as (after non-dimensionalisation) the following:

$$\begin{aligned} &C_{fx} = \left(\frac{1}{\sqrt{Re_x}}\right)\frac{d^2 f}{d\zeta^2}\Big|_{\zeta=0}, Nu_x = -\left(\sqrt{Re_x}\right)\frac{d\theta}{d\zeta}\Big|_{\zeta=0}, \\ &Sh_x = -\left(\sqrt{Re_x}\right)\frac{d\phi}{d\zeta}\Big|_{\zeta=0}. \end{aligned}$$

3. DESCRIPTION OF RESULTS

The reduced Eqs. (6) to (8) are nonlinear and coupled, and thus their exact analytical solutions are not possible. They can be solved numerically using Runge–Kutta– Fehlberg fourth fifth order method for different values of governing parameters. The effects of the emerging parameters on the dimensionless velocity, temperature, skin-friction, the rates of heat and mass transfer are investigated. The step size and convergence criteria were chosen to be 0.001 and 10^{-6}, respectively. The asymptotic boundary conditions in Eq (9) were approximated by using a value of 4 for ζ as follows: $\zeta_{max} = 4$. This ensures that all numerical solutions approached the asymptotic values correctly.

In order to get the group of Eqs. (6) to (8) based on the boundary conditions Eq. (9) are resolved via shooting approximation. Further, to judge the accuracy of reliable analysis, comparison with available results of Adegbie et al. [22] corresponding to coefficients (Table 1, Table 2 and Table 3) and found in good agreement. For numerical results, we considered the values to the non-dimensional parameters as

$$Pr = a_1 = a_2 = n = 1, M = Sc = S_t = m = \xi = 0.5,$$
$$Du = Sr = \beta = \delta = \gamma = 0.3, S_{sol} = 0.2.$$

These values are kept as common for the complete study unless otherwise they showed in the plots.

Figure 1 and Figure 2 elucidate the impact of M and S_t on velocity distribution. From Figure 1, it is manifest that one may discern that the values of M depreciates the velocity. The reason behind this Lorentz force has the tendency produced to strength of magnetic field. It is also observed that thermal stratification parameter intensifies velocity distribution due to wavy nature of the surface. In Figure 3 and Figure 4, the influence of Deborah number and temperature dependent viscous parameter on velocity profiles, it will manifest that for both cases velocity rises with evaluating values of β and ξ respectively. But the momentum boundary layer thickness for Figure 5 and Figure 6 are depressed with greater values of melting parameter *(m)* and temperature dependent thermal conductivity parameter (ε) due to heat flux on upper convicted Maxwell fluid flow characterization. It is apparent from Figures 7 and Figure 8, shows that the effect of Dufour number and velocity power index parameter on velocity profiles. From Figure7, it is dedicated that fluid velocities lessen with elevating values of *Du* . But velocity rises with higher values of power index parameter as shown in Figure 8.

It is evident from Figure 9 and Figure 10 the evaluation of M and S_t on temperature fields. It will manage that, magnetic parameter intensifies and thermal stratification parameter depressed for both cases of thermal boundary layer thickness of the flow system. Figure 11 and Figure 12 are designed to analyze the variation on temperature profile under the action of β and ξ .we will watch that increasing values of β and ξ leads to a down turn in the temperature thickness of one boundary layer. Figure 13 and Figure 14 are dedicated to know the effect of melting parameter *(m)* and temperature dependent thermal conductivity parameter (ε) on temperature profiles. We can understand that for both profile increasing turns with a gain in values of m and ε .

Figures 15 and Figure 16 reveals that *Du* raises and velocity power index parameter *n* downturns in the presence of velocity distribution for surrounding molecular as a consequence of decreases in fluid temperature. Figure 17 and Figure 18 render the temperature distribution of ascending values of Heat source parameter δ and soleted stratification parameter S_{sol}.

From Figure 19 and Figure 20 we reveals that boosting the values of δ and S_{sol} magnifies the thermal bounder layer thickness. Figure 21 and Figure 22 plot the effects of M, S_t, m, δ and ξ on skin friction coefficient. It will watch from Figure 23 r, S_t, δ depreciates and increases m, ε, ξ.

Figure 24 and Figure 25 depict the effects of $M, S_t, S_{sol}, \delta, \varepsilon$ and ξ on the non-dimensional Nusselt number .It will reveals that for all the parameters increases it will approach to the Nusselt number downwards for the specification of rate of rate of heat transfer respectively.Finally, Figure 26 and Figure 27 transmit that on enhancement in $\xi, \varepsilon, \delta, S_t$ and S_{sol} intensifies mass transfer rate(Sherwood number).

Owing to the advantage engineering applications, Table 4 exhibits the validation of the pertinent parameters on skin fiction coefficient, reduced Nusselt number and local Sherwood number for the parameters Dufour number, *(Du)*, Soret number *(Sr)* and thermal relaxation parameter (γ). This will say that all the aforementioned parameters except γ lessen the skin friction, Nusselt number coefficients and in reverse behavior in local Sherwood number respectively.

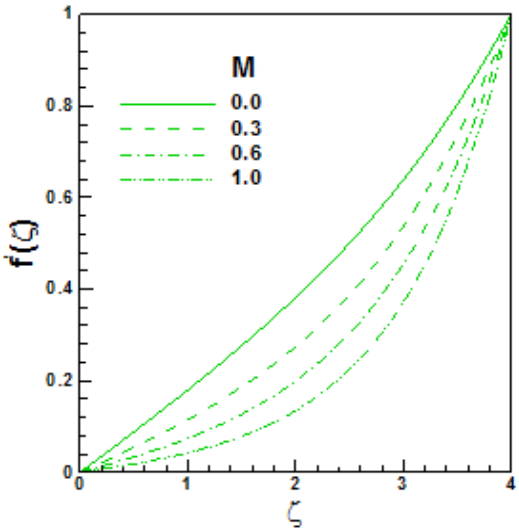

Figure 1. Effect of M on velocity

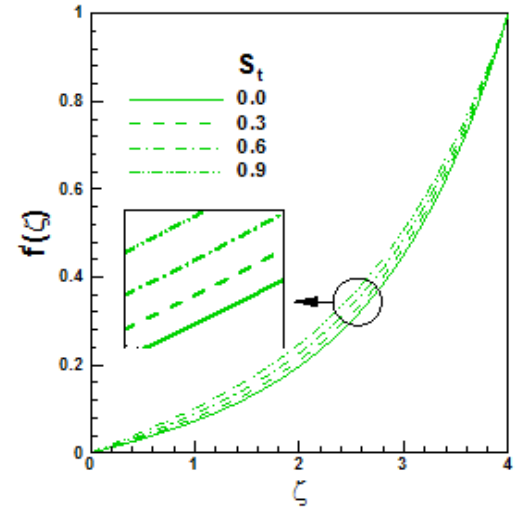

Figure 2. Effect of S_t on velocity

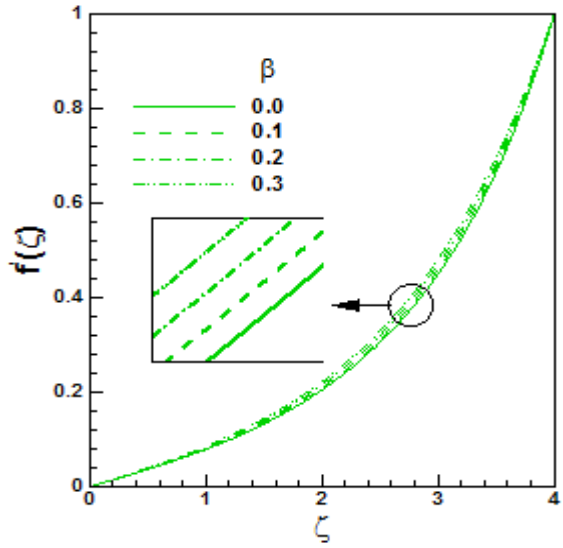

Figure 3. Effect of β on velocity

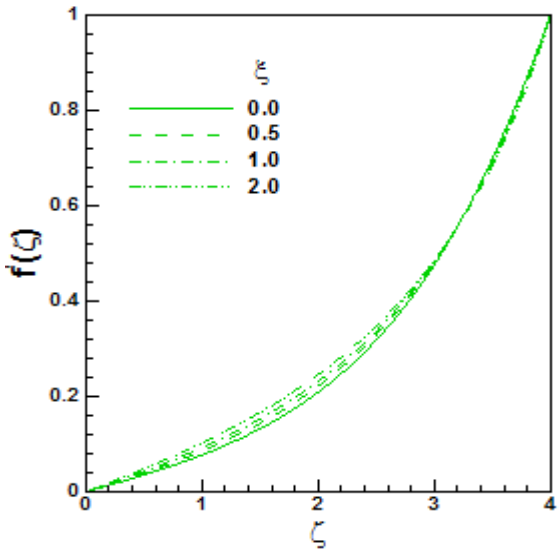

Figure 4. Effect of ξ on velocity

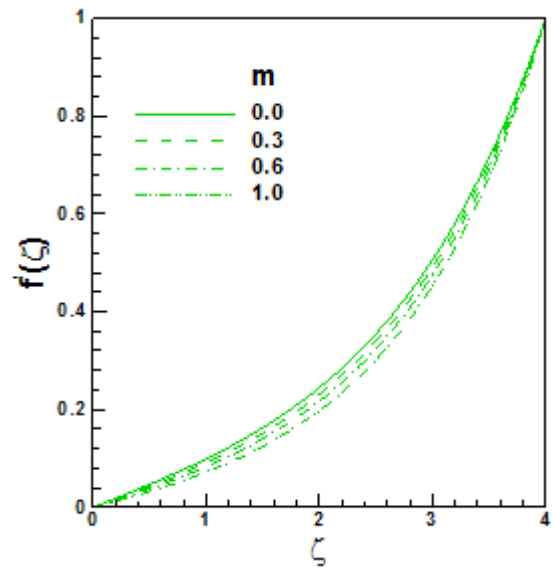

Figure 5. Effect of m on velocity

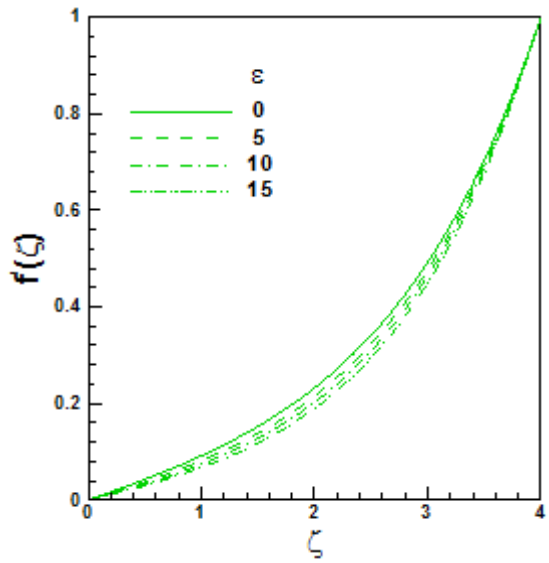

Figure 6. Effect of ε on velocity

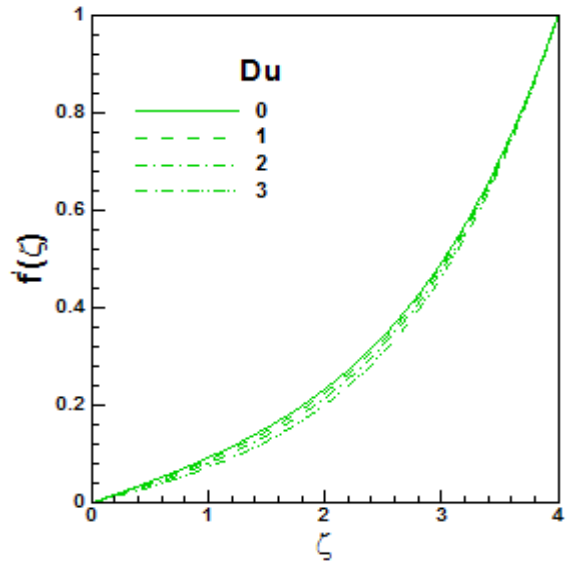

Figure 7. Effect of Du on velocity

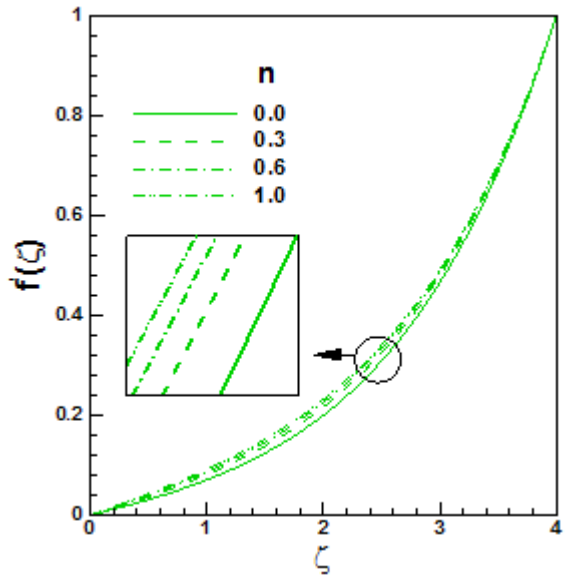

Figure 8. Effect of n on velocity

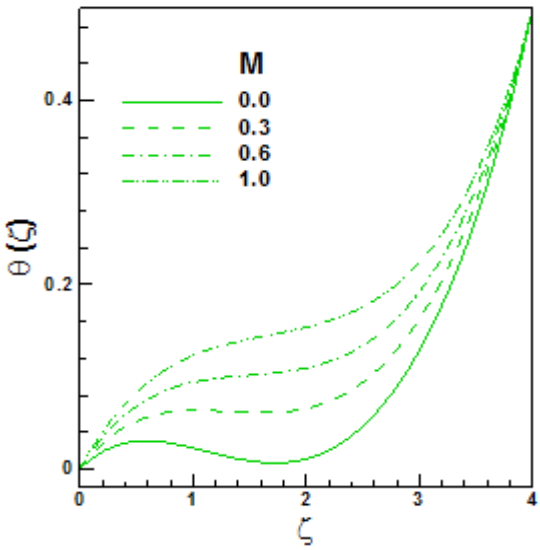

Figure 9. Effect of M on temperature

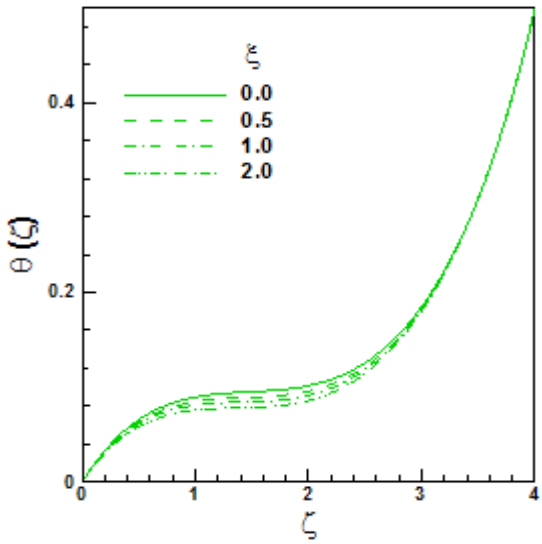

Figure 12. Effect of β on temperature

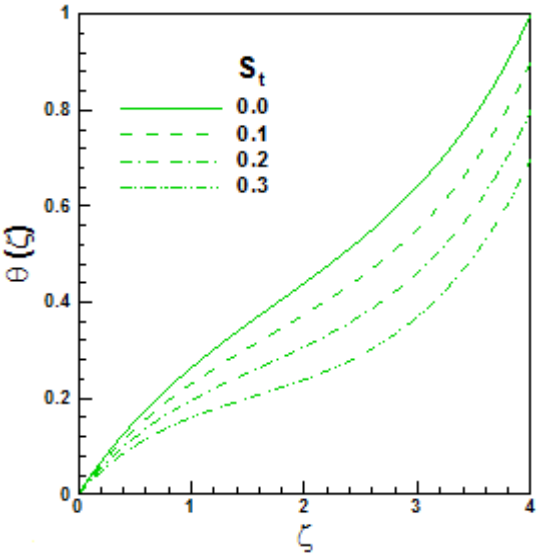

Figure 10. Effect of S_t on temperature

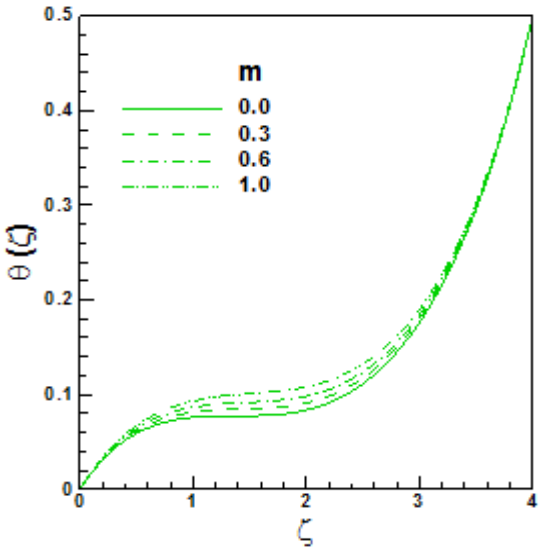

Figure 13. Effect of m on temperature

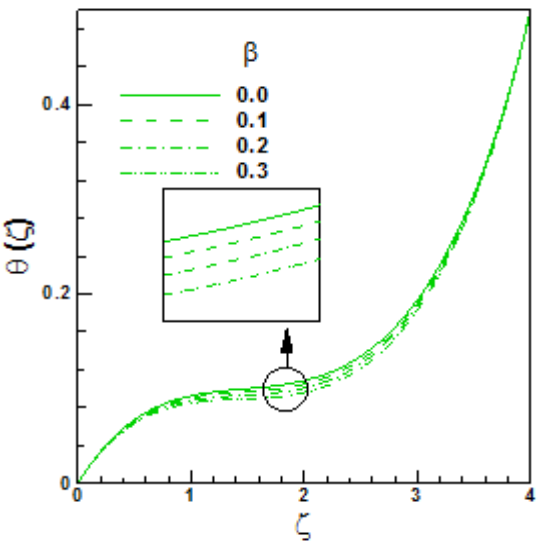

Figure 11. Effect of β on temperature

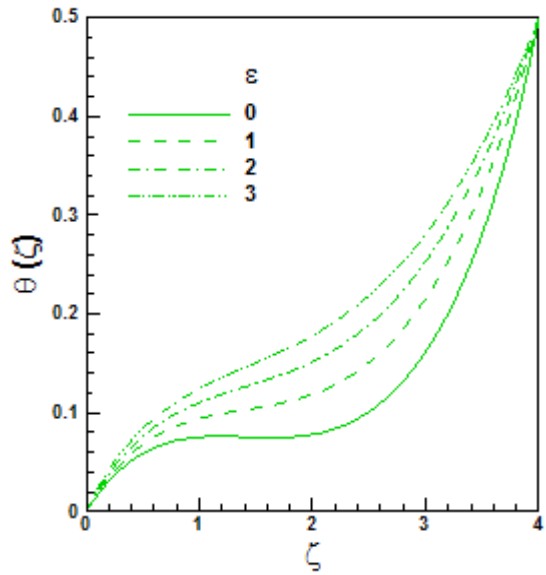

Figure 14. Effect of ε on temperature

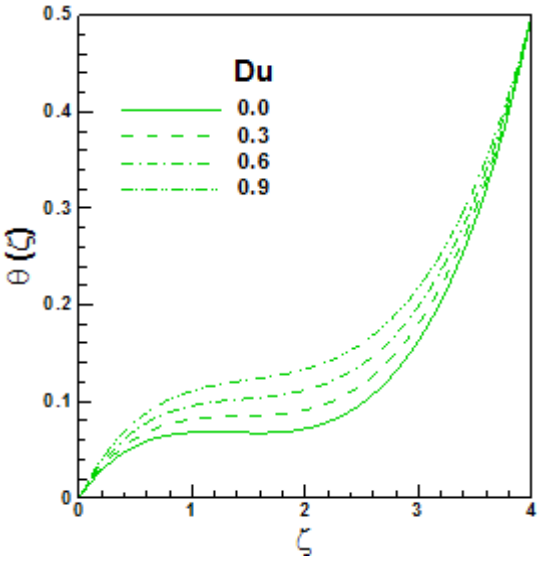

Figure 15. Effect of *Du* on temperature

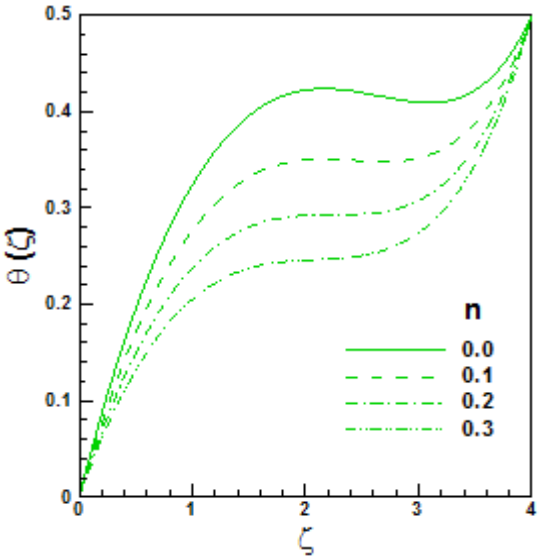

Figure 16. Effect of *n* on temperature

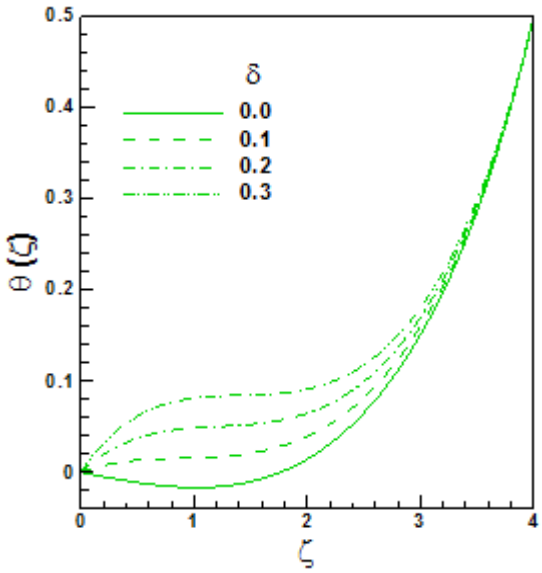

Figure 17. Effect of δ on temperature

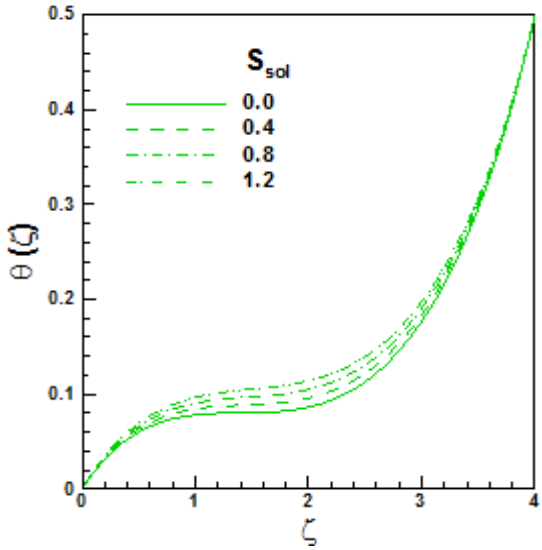

Figure 18. Effect of S_{sol} on temperature

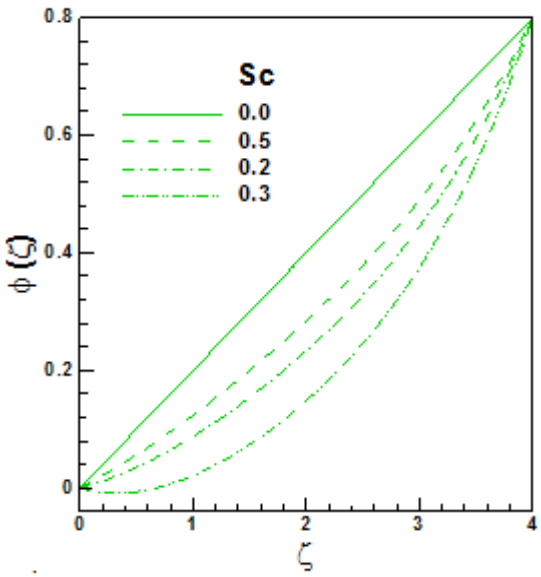

Figure 19. Effect of *Sc* on concentration

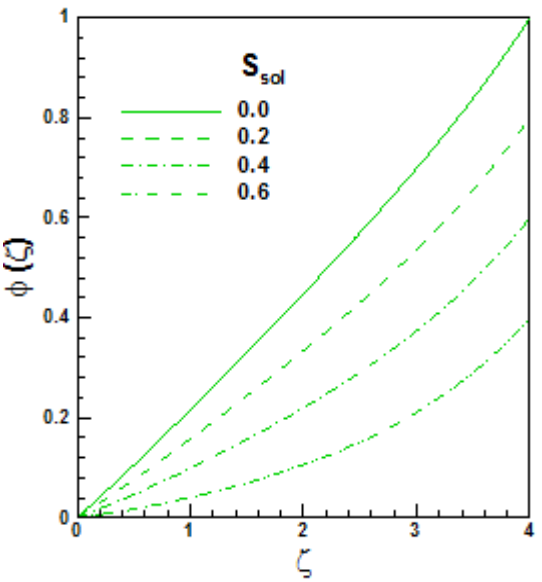

Figure 20. Effect of S_{sol} on concentration

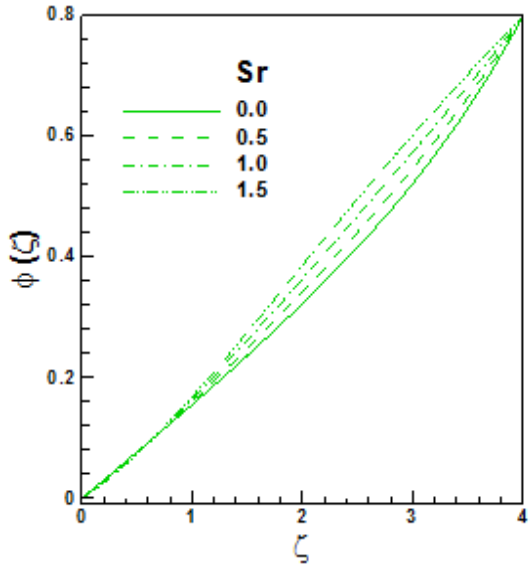

Figure 21. Effect of Sr on concentration

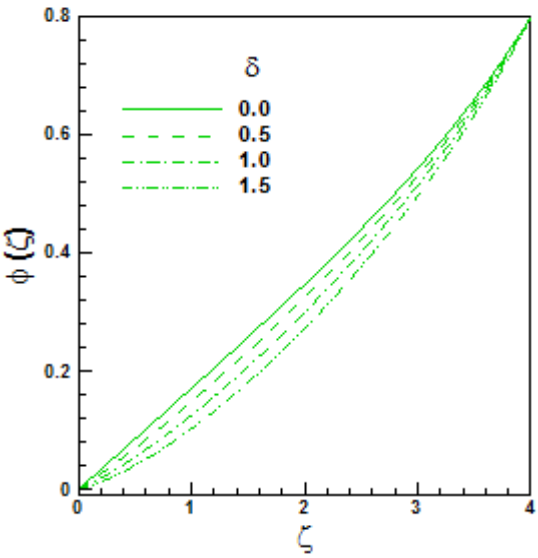

Figure 23. Effect of δ on concentration

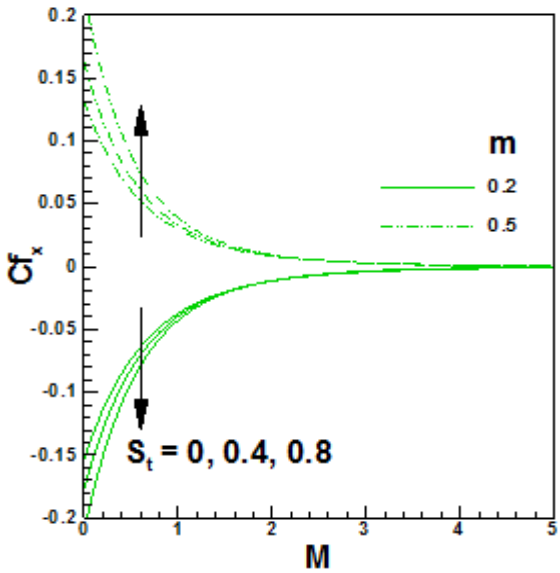

Figure 23. Effects of M, m, S_t on skin friction coefficient

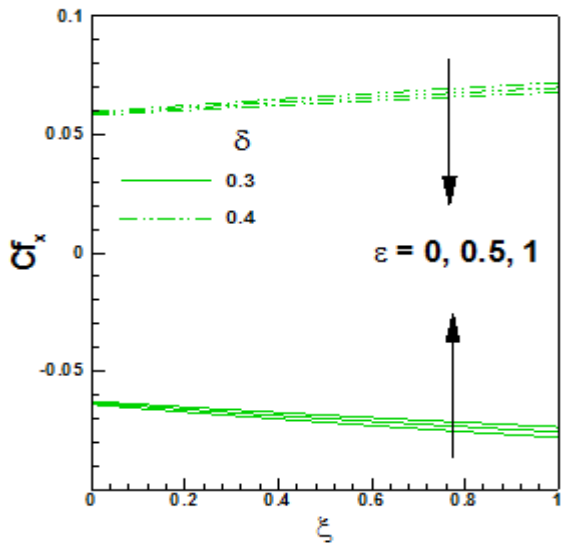

Figure 24. Effects of ξ, ε, δ on skin friction coefficient

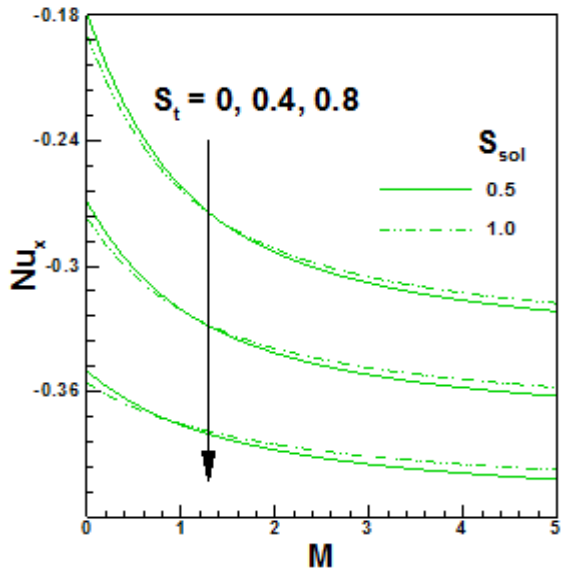

Figure 25. Effects of M, S_{sol}, S_t on Nusselt number

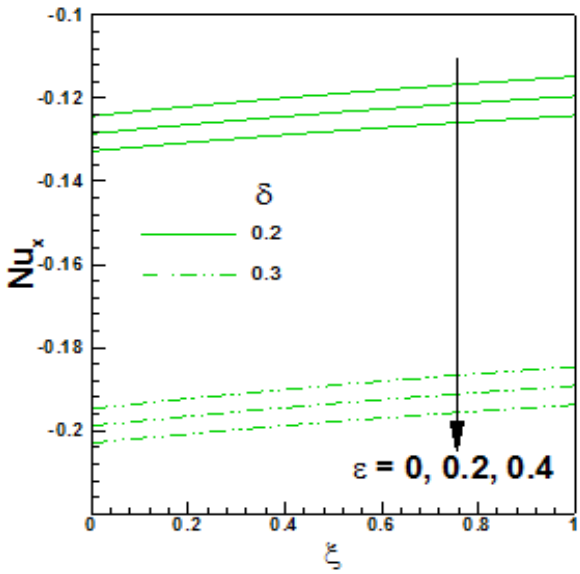

Figure 26. Effects of ξ, ε, δ on Nusselt number

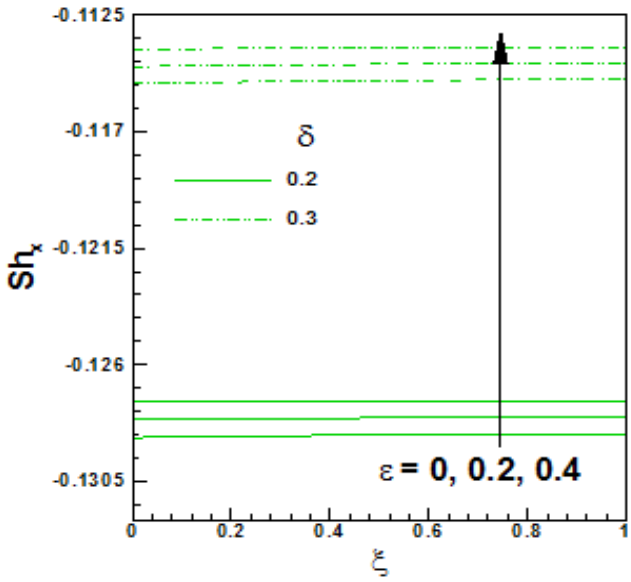

Figure 27. Effects of ξ,ε,δ on Sherwood number

Table 1. Comparison of $f''(0)$ when $Du=\gamma=Sr=0$.

Pr	m	Adegbie et al.[26]	Present
0.3	0	0.084750612582614	0.0847506307666679
0.5	0	0.085203475747002	0.0852034877663851
0.71	0	0.085590497630018	0.0855905106885111
1	0	0.086013790040591	0.0860138042003556
0.3	0.5	0.039237496643905	0.0392375059032759
0.5	0.5	0.054568458187466	0.0545684707127330
0.71	0.5	0.062316082253395	0.0623160827111398
1	0.5	0.067978247104503	0.0679782477002010

Table 2. Comparison of $-\theta'(0)$ when $Du=\gamma=Sr=0$.

Pr	m	Adegbie et al.[26]	Present
0.3	0	0.216400307739576	0.216400298274767
0.5	0	0.220822718730358	0.220822709690860
0.71	0	0.227973425611366	0.227973413333021
1	0	0.240922368071198	0.240922351912396
0.3	0.5	0.192839423367583	0.192839418011778
0.5	0.5	0.198631742945421	0.198631733315795
0.71	0.5	0.206753996042305	0.206753995597668
1	0.5	0.220488109991622	0.220488109364549

Table 3. Comparison of $-\phi'(0)$ when $Du=\gamma=Sr=0$.

Pr	m	Adegbie et al.[26]	Present
0.3	0	0.126425739785364	0.126425727304218
0.5	0	0.126353292670234	0.126353284497587
0.71	0	0.126290251750048	0.126290242936227
1	0	0.126219525847626	0.126219516353560
0.3	0.5	0.091023186146136	0.091023180441538
0.5	0.5	0.103581365442893	0.103581357632857
0.71	0.5	0.109309104668065	0.109309104360491
1	0.5	0.113210624587697	0.113210624201291

Table 4. Values of skin friction coefficient, Nusselt and Sherwood numbers when Pr=1.0, m=0.5, n=a_1=1, β=0.3, ξ=ε=S_t=δ=S_{sol}=0.2.

Du	Sr	γ	$f''(0)$	$-\theta'(0)$	$-\phi'(0)$
0.3	0.3	0.3	0.0667862	-0.2346408	-0.1024501
0.5			0.0654683	-0.2485729	-0.0996212
1			0.0619257	-0.2868486	-0.0918986
0.7	0.5		0.0634687	-0.2723217	-0.0837080
	0.8		0.0622125	-0.2903394	-0.0574314
	1		0.0610696	-0.3066567	-0.0331703
	0.7	0.5	0.0631164	-0.2805202	-0.0680090
		0.6	0.0634098	-0.2784038	-0.0685224
		0.7	0.0638094	-0.2755078	-0.0692664

4. CONCLUSIONS

Heat and mass transfer of the flow with Cattaneo-Christov heat flux on UCM cross a melting surface on the presence of double stratification and cross diffusion effects respectively. We assumed the normal stress and cross diffusion are of the same order of magnitude the main lists of the findings are as follows:

1. An increase in the thermal stratification parameter reduces the temperatures friction factor and local heat transfer coefficients but enhances velocity and local mass coefficients respectively.
2. Cross diffusion and double stratification effects are helpful to higher the motion of the fluid and regulate the heat and mass transfer rates.
3. The effect of the Dufour number is to reduce heat transfer and enhance mass transfer.
4. The effect of the Soret number is the exact opposite behavior of the Dufour effect.

In engineering areas, double diffusive convection has visualized in the form of fluid flows and metals surrounded by heat-diffusion fins.

REFERENCES

[1] Cattaneo C. (1948). Sulla conduzione del calore. Atti Semin. Mat. Fis. Univ. Modena Reggio Emilia 3 3: 83-101.

[2] Christov CI. (2009). On frame indifferent formulation of

the Maxwell-Cattaneo model of finite speed heat conduction. Mech. Res. Commun. 36(4): 481-486. https://doi.org/10.1016/j.mechrescm.2008.11.003
[3] Mustafa M. (2015). Cattaneo-Christov heat flux model for rotating flow and heat transfer of upper-convected Maxwell fluid Cattaneo-Christov heat flux model for rotating flow and heat transfer of upper-convected Maxwell fluid. AIP. Adv. 5(4): 047109. https://doi.org/10.1063/1.4917306
[4] Hayat T, Qayyum S, Imtiaz M, Alsaedi A. (2016). Three-dimensional rotating flow of Jeffrey fluid for Cattaneo-Christov heat flux model. AIP. Adv. 5(2): 025012. https://doi.org/10.1063/1.4942091
[5] Tanveer A, Hina S, Hayat T, Mustafa M, Ahmad B. (2015). Effects of the Cattaneo–Christo heat flux model on peristalsis. Eng. Appl. Comp. Fluid Mech. 10(1): 373-383. https://doi.org/10.1080/19942060.2016.1174889
[6] Khan JA, Mustafa M, Hayat T, Alsaedi A. (2015). Numerical study of Cattaneo-Christov Heat flux model for viscoelastic flow due to an exponentially stretching surface. PLOS ONE 10(9): 0137363. https://doi.org/10.1371/journal.pone.0137363
[7] Han S, Zheng L, Li C, Zhang X. (2014). Coupled flow and heat transfer in viscoelastic fluid with Cattaneo-Christov heat flux model. Appl. Math. Lett. 38: 87-93. https://doi.org/10.1016/j.aml.2014.07.013
[8] Waqas M, Hayat T, Farooq M, Shehzad, S. A., Alsaedi, A. (2016). Cattaneo-Christov heat flux model for flow of variable thermal conductivity generalized Burgers fluid. Journal of Molecular Liquids 220: 642-648. https://doi.org/10.1016/j.molliq.2016.04.086
[9] Hayat T, Qayyum S, Imtiaz M, Alsaedi A. (2016). Impact of Cattaneo-Christov heat flux in Jeffrey fluid flow with homogeneous-heterogeneous reactions. PLOS ONE 11(2): 0148662. https://doi.org/10.1371/journal.pone.0148662
[10] Straughan B. (2010). Thermal convection with the Cattaneo-Christov model. Int. J. Heat Mass Transf. 53(1-3): 95-98. https://doi.org/10.1016/j.ijheatmasstransfer.2009.10.001
[11] Huppert HE, Sparks RSJ. (1984). Double-diffusive convection due to crystallization in magmas. Annu. Rev. Earth Planet. Sci. 12: 11-37. https://doi.org/10.1146/annurev.ea.12.050184.00303
[12] Fernando, H. J. S., Brandt, A. (1994). "Recent advances in double-diffusive convection," Appl. Mech.Rev. 47: c1-c7.
[13] Akbarzadeh A, Manins P. (1988). Convective layers generated by side walls in solar ponds. Sol. Energy 41(6): 521-529. https://doi.org/10.1016/0038-092X(88)90055-2
[14] Narayana M, Sibanda P, Motsa SS, Siddheshwar PG. (2012). On double-diffusive convection and cross diffusion effects on a horizontal wavy surface in a porous medium. Boundary Value Problems 2012: 1-22. https://doi.org/10.1186/1687-2770-2012-88
[15] Srinivasacharya D, Surender O. (2015). Effect of double stratification on mixed convection boundary layer flow of a nano-0fluid past a vertical plate in a porous medium. Appl. Nanosci. 5(1): 29-38. https://doi.org/10.1007/s13204-013-0289-7
[16] Narayana M, Sibanda P, Motsa SS, Lakshmi-Narayana PA. (2012). Linear and nonlinear stability analysis of binary Maxwell fluid convection in a porous medium. Heat Madd Transf. 48(5): 863-874. https://doi.org/10.1007/s00231-011-0939-9
[17] Malashetty MS, Biradar BS. (2011). The onset of double diffusive convection in a binary Maxwell fluid saturated porous layer with cross-diffusion effects. Phys. Fluids 23(6): 064102. https://doi.org/10.1063/1.3601482
[18] Chamkha AJ, Abdulgafoor F. (2006). Double-diffusive convection in a titled enclosure filled with a non-Darcian porous medium. Heat and Technology 24(1): 141-152. https://doi.org/10.18280/ijht.240118
[19] Nasrina R, Alim MA. (2012). Soret and Dufour effects on double diffusine natural convection in a chamber utilizing nanofluid. International Journal of Heat and Technology 30(1): 109-118. https://doi.org/10.18280/ijht.240107
[20] Ghernaout B, Bouabdallah S, Teggar M, Benniche H. (2015). Double diffusive natural convection in binary mixture under the effect of external magnetic field: stedy and oscillatory state. International Journal of Heat and Technology 33(4): 11-18. https://doi.org/10.18280/ijht.330402
[21] Raju CSK, Ibrahim SM, Anuradha S, Priyadharshini P. (2016). Bio-convection on the nonnlinear radiative flow of a Carreau fluid over a moving wedge with suction or injection. The Er. Phys. J. Plus. 131. https://doi.org/10.1140/epjp/i2016-16409-7
[22] Raju CSK, Sekhar KR, Ibrahim SM, Lorenzini G, Viswanatha Reddy G, Lorenzini E. (2017). Variable viscosity on unsteady dissipative Carreau fluid over a truncated cone filled with titanium alloy nanoparticles. Continuum Mech. Thermodyn. 29(3): 699-713. https://doi.org/10.1007/s00161-016-0552-8
[23] Ibrahim W, Makinde OD. (2016). Magnetohydrodynamic stagnation point flow and heat transfer of Casson nanofluid past a stretching sheet with slip and convective boundary condition. J. Aerospace. Eng. 29(2). https://doi.org/10.1061/(ASCE)AS.1943-5525.0000529
[24] Ibrahim W, Makinde OD. (2016). Magnetohydrodynamic stagnation point flow of a power-law nanofluid towards a convectively heated stretching sheet with slip. in Proceedings of the Institution of Mechanical Engineers, Part E: Journal of Process Mechanical Engineering, pp. 345-354.
[25] Adegbie KS, Ommowaye AJ, Disu AB, Animasaun IL. (2015). Heat and mass transfer of upper convected Maxwell fluid flow with variable thermo-physical properties over a horizontal melting surface. Applied Mathematics 6: 1362-1379. https://doi.org/10.4236/am.2015.68129

NOMENCLATURE

a_1, b_1, a_2, b_2	dimensional constants
a	stretching rate, s^{-1}
B	Dimensional magnetic field parameter
x, y	Directions along and normal to the surface, m
u, v	velocity components along $x \& y$ directions, $m.s^{-1}$
T_m	dimensional thermal stratification
C_m	dimensional solutal stratification

T_0	reference temperature, K
C_0	reference concentration, kg.m^{-3}
T	temperature of the fluid, K
C_p	specific heat capacity at constant pressure, J. kg^{-1}. K^{-1}
Q_0	heat generation/absorption parameter
D_m	molecular diffusivity of the species concentration
k_T	thermal diffusion ratio
C_s	concentration susceptibility, kg.m^{-3}
C	concentration of the fluid, kg.m^{-3}
S_t	thermal stratification parameter
n	velocity power index parameter
S_{sol}	solutal stratification parameter
k	thermal conductivity W.m^{-1}. K^{-1}
m	melting parameter
f	dimensionless velocity
M	magnetic field parameter
Pr	prandtl number
Du	dufour number
Sc	schmidt number
Sr	soret number
C_{fx}	local skin friction coefficient
Nu_x	local Nusselt number
Sh_x	local Sherwood number
Re_x	local Reynolds number

Greek symbols

λ^*	latent heat of the fluid
λ	dimensional viscoelastic parameter
β	deborah number
ρ	electrical conductivity of the fluid, W.m^{-1}.K^{-4}
σ	density of the fluid, Kg.m^{-1}
ϕ	dimensionless concentration
ζ	similarity variable
δ	heat source parameter
θ	dimensionless temperature
μ	dynamic viscosity, kg. m^{-1}.s^{-1}
ν	kinematic viscosity, m^2.s^{-1}
ξ	temperature dependent viscous parameter
ε	temperature dependent thermal conductivity parameter
γ	thermal relaxation parameter